Journal of the Southeastern Association for Research in Astronomy, **7**, 13-16, 2012 December 1


# OPTICAL MONITORING OF THREE ACTIVE GALACTIC NUCLEI

Michelle A. Berg[1,2]
Department of Physics and Space Sciences, Florida Institute of Technology, Florida, 32901

Kyle F. Twadelle[1,2]
Department of Astronomy, University of Michigan, Ann Arbor, Michigan, 48109

and

Daniel Batcheldor
Department of Physics and Space Sciences, Florida Institute of Technology, Florida, 32901

## ABSTRACT

The dusty torus is the centerpiece of the Unified Model of Active Galactic Nuclei (AGN), but its size and dust distribution is unknown. Observations of three galaxies, MRK 885, NGC 6418, and 3C 390.3, with AGN were conducted in the optical wavelengths ($B$ and $V$ bands) over a four night period to constrain the optical variability of the AGN. Absolute photometry was unable to be used for the data collected due to non-photometric nights and uncertainty in the photometric zero points, so differential photometry was used instead. MRK 885 and NGC 6418 showed no change in magnitude over four nights, but 3C 390.3 showed a decrease in brightness in only one filter. Linear regression was performed on the light-curves for each galaxy, and it was concluded that the change in brightness, if real, was not statistically significant.

*Subject headings:* dusty torus, active galactic nuclei, monitoring, optical fluxes, infrared

## 1. INTRODUCTION

The Unified Theory of Active Galactic Nuclei (AGN) hinges on a dusty torus that lies around a Broad-Line Region (BLR), located around the accretion disk of the supermassive black hole (SMBH) at the center of the galaxy, and has an extended Narrow-Line Region (NLR) positioned above and below the torus. Depending on the viewing angle of the observer to the galaxy, the BLR might be obscured. AGN that are viewed edge-on where only the NLR can be seen are classified as Seyfert 2 galaxies, while those that are viewed face-on, showing both the BLR and NLR, are called Seyfert 1 galaxies, though they are essentially the same. For example, see (Barvainis 1987; Axon 2001; Li 2008).

The obscuring region, which does not always align with its host galaxy's axis, is thick and opaque, most likely consisting of clumps of gas and dust rather than a smooth distribution (Barvainis 1987; Kawaguchi & Mori 2011). It is perhaps shaped like a doughnut and made from dust clouds that are accreted from the galaxy, containing graphite grains rather than silicates (Barvainis 1987; Clavel et al. 1989; Elitzur 2006). Even though current telescopes are unable to spatially resolve the torus, evidence of dust in this region is seen through spectropolarimetry, spectroscopy, reverberation mapping, and time variability (Rodríguez-Ardila & Mazzalay 2006; Li 2008; Kawaguchi & Mori 2011; Fine et al. 2012).

What is unknown about the dusty torus is how far it extends and if it has a smooth or clumpy distribution. A relation between the inner radius of the torus using the sublimation temperature of the dust clumps and observations of near-infrared reverberation from the dust was discovered by Barvainis (1987). The critical temperature of ∼1500 K is where the dust clumps in the torus would sublimate (Kawaguchi & Mori 2011). Previous observations have shown the torus to be no more than a few parsecs wide, with the hot dust located inside a radius of four parsecs (Elitzur 2006; Rodríguez-Ardila & Mazzalay 2006; Nenkova et al. 2008a,b). Conversely, Fairall 9, which was studied by Clavel et al. (1989), has its BLR ∼.13 parsecs from the dust shell. 3C 390.3 has been calculated to have its BLR at a distance of .042 parsecs from the dust shell (Dietrich et al. 2010).

For this study, the time variability of a galaxy's light curves in the optical wavelengths from ground based observations using the 0.9m Southeastern Association for Research in Astronomy (SARA) telescope at Kitt Peak National Observatory (KPNO) will be compared to the galaxy's light curves at the infrared wavelengths of 3.6$\mu$m and 4.5$\mu$m through the Spitzer Space Telescope. Through comparing the light curves and possible time delay ranges between an event in the optical and infrared, the temperature and spatial distribution of the dust can be estimated (Clavel et al. 1989).

Time lags have already shown that differences between the ultraviolet and infrared are due to re-emission from dust (Suganuma et al. 2007). A longer delay in the light curves can be caused by a larger inclination angle of the galaxy, a misaligned torus, a larger torus size, or reverberations from dust clumps within the torus (Kawaguchi & Mori 2011). Because the distribution of the dust grains most likely varies with the torus radius, the infrared observations are being taken at two different wavelengths. The wavelengths chosen are under 25$\mu$m to prevent con-

[1] Southeastern Association for Research in Astronomy (SARA) NSF-REU Summer Intern
[2] Visiting observer, SARA Observatory at Kitt Peak, Arizona, which is operated by the Southeastern Association for Research in Astronomy
Electronic address: mberg2010@my.fit.edu

TABLE 1
Target Information[a]

| Object | Type | $B$ | $V$ |
|---|---|---|---|
| MRK 885 | S 1.5 | 15.4 | 14.5 |
| NGC 6418 | S 1 | 16.0 | 15.2 |
| 3C 390.3 | S 1.5 | 15.6 | 15.0 |

[a]The information for the galaxies was take from the NASA/IPAC Extragalactic Database (NED).

TABLE 2
Observations

| Object | Filter | Exposure (s) | Images |
|---|---|---|---|
| MRK 885 | $B$ | 120 | 20 |
| | $V$ | 50 | 15 |
| NGC 6418 | $B$ | 60 | 15 |
| | $V$ | 30 | 20 |
| 3C 390.3 | $B$ | 30 | 20 |
| | $V$ | 30 | 20 |

tamination from foreground dust (Axon 2001).

In Section 2, the observations and instruments used will be discussed, followed by the data reduction process in Section 3. The results of these observations will then be described in Section 4, and then a discussion in Section 5 to possibly link an infrared reverberation mapping of the torus to this optical monitoring study. Section 6 concludes.

## 2. OBSERVATIONS

All observations of the standard star, GSC 04198-01768, and the galaxies, MRK 885, NGC 6418, and 3C 390.3, were taken at the SARA North 0.9m telescope at KPNO over a four night period from June 16, 2012 through June 19, 2012. Each galaxy was observed once every night and the standard star was observed first at the beginning of the night, between each galaxy observation, and also at the end of each night. The observations were taken consecutively. The standard star is an A0 type star with a $B$ magnitude of 9.72 and a $V$ magnitude of 9.65.

All of the objects were observed with the $B$ and $V$ filters, and the images were taken with an Apogee charge-coupled device (CCD). Each observation of the standard star had a 3 second exposure in the $B$ filter for 5 images, and a 2 second exposure with the $V$ filter for another 5 images. Standard calibration images were also taken, and the telescope was dithered for the observations of the galaxies to allow removal of hot pixels and cosmic rays.

See Table 1 for a description of the targets and Table 2 for a description of the observations taken.

## 3. DATA REDUCTION

After the observations were taken, the images needed to be preprocessed before any information could be extracted from them. Each night's images were treated separately, except for the calibration images. The CCD cooler had not reached its set point for two of the nights' bias frames, causing their bias levels to be too high; the bias frames of the nights the cooler was at its set point were reused for these nights. Dark frames were also taken only twice and were reused for the other nights. Flat fields were unable to be taken the first night, so the flat fields taken the next night were used instead.

Through using the standard packages in the Image Reduction and Analysis Facility (IRAF), for each night, the bias frames were median combined, and the master bias was then subtracted from the dark frames. The dark frames were then median combined as well. The master dark was divided by the dark frame exposure time to obtain the dark rate. The master bias was then subtracted from the flat fields, and the dark rate was multiplied separately by the exposure time of the flat fields. This flat field dark rate was subtracted from the flat fields, and the flat fields were then normalized. For the individual filters, the flat fields were then median combined to create a master flat field.

Once the calibration images were readied, the images were then preprocessed. The master bias was subtracted from all of the appropriate images, and then the images were divided by the master flat field. After the images had been calibrated, they were aligned using IRAF. The alignment was done by calculating pixel offsets in $x$ and $y$ using the centroid position of 3 stars common to each field, and then shifting each image to a common position on the detector. The images were then median combined by filter. Through the IRAF `apphot` package and `phot` task and the technique of aperture photometry, the total counts and uncertainty for the standard star and galaxies were gathered using a radius of five pixels. This radius was chosen because that is where the point-spread function of the objects leveled off.

Because the images were taken at different air masses, the light-curves needed to be adjusted for atmospheric extinction. The air masses of the standard star were the first to be calculated. As the air mass decreases the total counts for the star should increase. Upon comparing the standard star's air mass to its counts, this was not the case. The aperture photometry was then repeated at a radius of eight pixels to make sure all of the star was being included inside the aperture. The average air mass, average total counts, and standard deviation of the counts were then calculated individually for each filter and for each time the star was observed.

A trend line was fit to the graphs of the average radius verses the average counts for each filter for each night. The result, if the night was photometric, should be a linear, negatively sloping line. The graphs showed that the 19th was not photometric and that the 16th was not photometric in the $B$ band; this data was then discarded. It is possible that the use of the calibration images from other nights affected these images, but some nights with reused calibration images were photometric. Going forward with the resultant data, the photometric zero point of the standard star and its uncertainty were then calculated for each filter for each night using the equation:

$$m = -2.5\log(F) + Z \quad (1)$$

where $m$ is the magnitude of the standard star for a specific filter, $F$ is the maximum counts of the star outside of the earth's atmosphere (y-intercept of the trend line), and $Z$ is the photometric zero point. The relative uncertainties in the zero points were 83% of the zero point. Since no consistent results could be obtained from the standard star, differential photometry was used instead.

Because differential photometry focuses on each image individually, all of the data, even from the non-photometric nights could be used. The standard star data was no longer needed because five comparison stars were selected in each image field to determine if there was a change in the galaxy's brightness. The five comparison stars used for each galaxy were the same for each night in each filter and were all brighter than the galaxy.

Aperture photometry was again used for the galaxy and the five comparison stars with a radius of five pixels to obtain their maximum counts and uncertainty. Pogson's equation, where $\Delta m$ is the difference in magnitude, $F_1$ is the galaxy's maximum counts (treated by filter and night separately), $F_2$ is the comparison star's maximum counts (treated by filter and night separately) was used to find the difference in magnitude between the comparison stars and the galaxy. Once the differences were calculated, the first night's $\Delta m$'s for each galaxy in each filter became the zero-point. The difference between the other three nights' $\Delta m$'s and the zero-point were then calculated with uncertainty. The magnitude differences of the four nights verses modified Julian Date were then graphed for each galaxy in each filter.

## 4. RESULTS

Upon analyzing the light-curves, MRK 885 and NGC 6418 showed no significant change on a timescale of four nights. 3C 390.3 in the $B$ filter also was unchanged, but in the $V$ filter, on the third night of observing, there is a potential change in magnitude. Because this magnitude change is only seen in the $V$ band, it is likely that this is spurious. This will be discussed further in Section 5.

The error bars on the graphs are very large for the second and fourth nights of observing. This is due to a telescope malfunction. The worm gear that controls the right ascension for the telescope was still rolling even when the system had deemed the telescope's position to be locked. The stars in the images for those two nights have long trailing tails. These tails and the non-symmetrical shape of the stars contribute to the large uncertainty in the counts and magnitude differences.

The error bars are also greater in the $B$ band than in the $V$ band because after roughly five minutes of observations the gear would then lock into place. The $B$ filter was used to observe the objects first, and when the filter was switched to $V$, the gear was then in place.

A second reason why there are large error bars for the second and fourth nights of observing is because those two nights were extremely windy. The error bars on the graphs for the fourth night are larger than those for the second night because that night had higher wind speeds, creating even longer tails on the stars in the images.

See Figures 1, 2, and 3 for the graphs of the light-curves of the galaxies.

## 5. DISCUSSION

Linear regression was performed on each light-curve and the uncertainty in the coefficient (slope) of the lines were all nearly zero. These uncertainties show the linear regressions to be consistent with horizontally straight lines, meaning that there was no change in magnitude for either galaxy over the four night period. The magnitude change in the $V$ band graph of 3C 390.3, if it is real, is not a significant enough change to claim there was a change

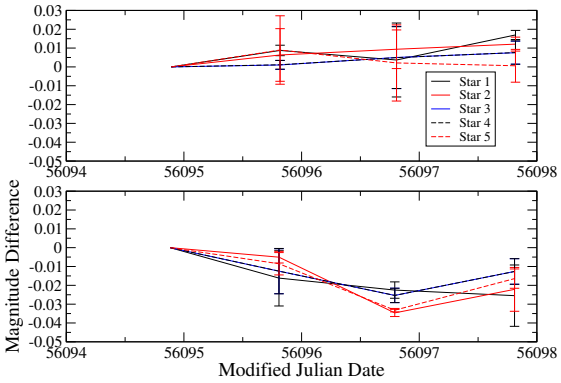


FIG. 1.— This light-curve is of the galaxy 3C 390.3. (*top panel*) $B$ band data. (*bottom panel*) $V$ band data. Please note that Star 3 and Star 4 are indistinguishable from each other on the graph.

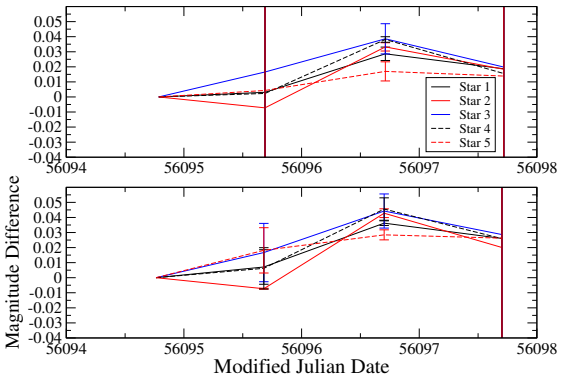


FIG. 2.— This light-curve is of the galaxy MRK 885. (*top panel*) $B$ band data. (*bottom panel*) $V$ band data.

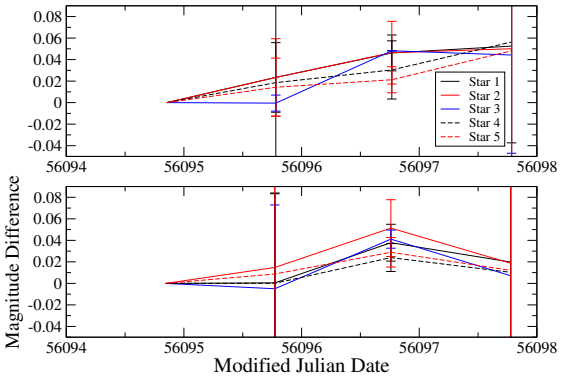


FIG. 3.— This light-curve is of the galaxy NGC 6418. (*top panel*) $B$ band data. (*bottom panel*) $V$ band data.

in brightness for that galaxy. This result is consistent with long term observations of 3C 390.3 which found a 1.5 magnitude change over a ten year period (Roberts & Rumstay 2012).

If the galaxies' spectra was also taken, the difference between the light-curves and the spectrum could have been compared to the transfer function. The transfer function is a nonlinear function that shows the time delays and structure of an observed object (Peterson 2001). The emitting region that was observed in this study is most likely the accretion disks of these AGN. Because the spectra of these galaxies were not taken, conjectures about the shape of the accretion disks cannot be made.

What can be concluded from this data is that the accretion disk must be at least greater than 690 AU across.

TABLE 3
Optical Magnitude Changes

| Object | Filter | Uncertainty |
|---|---|---|
| 3C 390.3 | $B$ | 0.00037 |
| | $V$ | 0.0057 |
| MRK 885 | $B$ | 0.0047 |
| | $V$ | 0.0052 |
| NGC 6418 | $B$ | 0.0074 |
| | $V$ | 0.0073 |

[a]The third column is the uncertainty in the coefficient (slope) taken from the linear regressions. The trend lines are horizontal lines.

TABLE 4
Infrared Magnitude Changes

| Object | Channel ($\mu$m) | IR Slope |
|---|---|---|
| 3C 390.3 | 3.6$\mu$m | 0.000235 |
| | 4.5$\mu$m | 0.000204 |
| MRK 885 | 3.6$\mu$m | ··· |
| | 4.5$\mu$m | ··· |
| NGC 6418 | 3.6$\mu$m | 0.00269 |
| | 4.5$\mu$m | 0.00129 |

[a]This information is pertaining to an infrared study of these same objects. The channels, as mentioned in the introduction, are the two infrared wavelengths used to observe the objects.
[b]The third column is the expected change in galaxy brightness over a period of 4 nights using the infrared data. MRK 885 showed no change in the infrared study over a year, so there was no slope to be calculated.

The SMBH at the center of 3C 390.3 has been calculated to be $2\times10^9$ $M_\odot$(Sergeev et al. 2011). We calculated its Schwarzschild radius to be 39.44 AU, which is much smaller than our limit on the accretion disk. Upon calculating the photon sphere to be 0.00029 parsecs, we see that this region is found at the edge of the black hole and not in the BLR.

Twadelle et al. (2012) conducted research on the same galaxies and standard star as this study, but at two infrared wavelengths. The data was taken for a year and did not include the dates of this optical study. Because the observations dates differ, no correlations from the data sets can be made, but the expected change in magnitude for the galaxies over a four night period can be estimated from the Twadelle et al. (2012) data.

By fitting a linear regression between the minimum and maximum points of half a period, the average change in brightness of the galaxy over six months can be calculated. Converting that result from months into days and then multiplying by four days, gives the expected change in the galaxy over a four night period. These four-night slopes were decimals that went to the hundredth and thousandth place for a positive integer, showing that there is little change expected over so short a period of observations. The uncertainties in the coefficient (slope) from the optical data are consistent with the calculated four-night slopes from the infrared data.

Tables 3 and 4 gives more information about the magnitude changes of the optical and infrared data over four nights.

## 6. CONCLUSIONS

Over the four night period that these observations were taken, none of the galaxies showed any significant changes in the brightness of their AGN. All of the light-curves were able to have a horizontal linear trend line fit to the data, and by using the infrared data from Twadelle et al. (2012) the estimated magnitude change for a four night period was calculated. This estimation was consistent with the optical findings of no significant changes in the AGN magnitudes over so short a period. We find that any optical variations in these targets must be coming from a region bigger than 690 AU. In future observations an elliptical aperture could be used to bypass the worm gear malfunction.

This project was funded by the National Science Foundation Research Experiences for Undergraduates (REU) program through grant NSF AST-1004872. This research has made use of the NASA/IPAC Extragalactic Database (NED) which is operated by the Jet Propulsion Laboratory, California Institute of Technology, under contract with the National Aeronautics and Space Administration.

## REFERENCES

Axon, D. J. 2001, The Central Kiloparsec of Starbursts and AGN: The La Palma Connection, 249, 193
Barvainis, R. 1987, ApJ, 320, 537
Clavel, J., Wamsteker, W., & Glass, I. S. 1989, ApJ, 337, 236
Dietrich, M., Peterson, B. M., & Grier, C. 2010, Bulletin of the American Astronomical Society, 42, #433.23
Elitzur, M. 2006, New Astronomy Review, 50, 728
Fine, S., Shanks, T., Croom, S. M., et al. 2012, arXiv:1205.1401
Kawaguchi, T., & Mori, M. 2011, ApJ, 737, 105
Li, A. 2008, arXiv:0808.4117
Nenkova, M., Sirocky, M. M., Ivezić, Ž., & Elitzur, M. 2008a, ApJ, 685, 147
Nenkova, M., Sirocky, M. M., Nikutta, R., Ivezić, Ž., & Elitzur, M. 2008b, ApJ, 685, 160
Peterson, B. M. 2001, Advanced Lectures on the Starburst-AGN, 3
Roberts, C. A., & Rumstay, K. R. 2012, Journal of the Southeastern Association for Research in Astronomy, 6, 47
Rodríguez-Ardila, A., & Mazzalay, X. 2006, MNRAS, 367, L57
Sergeev, S. G., Klimanov, S. A., Doroshenko, V. T., et al. 2011, MNRAS, 410, 1877
Suganuma, M., Kobayashi, Y., Yoshii, Y., et al. 2007, The Central Engine of Active Galactic Nuclei, 373, 462
Twadelle, K. F., Berg, M. A., & Batcheldor, D. 2012, JSARA, 7, 17